Adsorption of a Hydrophobically Modified Polysaccharide at the Air−Water Interface: Kinetics and Structure

Bruno Demé[†] and Lay-Theng Lee*[,‡]

Service de Chimie Moléculaire, C.E. Saclay, 91191 Gif sur Yvette Cedex, France Laboratoire Léon Brillouin, CEA-CNRS, C. E. Saclay, 91191 Gif sur Yvette Cedex, France

Received: April 28, 1997[⊗]

We have used specular neutron reflectivity to study adsorbed layers of a modified polysaccharide bearing lateral cholesterol anchors (cholesterylpullulan, CHP) at the air−water interface. In this system, the otherwise non surface active polysaccharide is attached, at several points along the backbone, to the surface by the hydrophobic cholesterol groups. The properties of these adsorbed polymer layers have been studied for different degrees of cholesterol substitution varying from 0.6 to 1.4 mol % and for different bulk concentrations. Using a parabolic profile to describe the adsorbed layer, it is found that the thickness of the layer decreases with surface concentration. These results are in contrast to those reported for end-attached tethered polymer layers. We attribute this behavior to the associative properties of the polymer as the interacting cholesterol groups are increased in the layer. Furthermore, the amount of polymer adsorbed decreases with the degree of cholesterol substitution. Surface tension data show that very long equilibration times are required for the formation of the polymer layers at the surface. However, the neutron reflectivity data show that even though the concentration profile changes over time, the amount of polymer adsorbed remains constant. These results suggest that the slow kinetics observed in surface tension measurements are due to structural rearrangements in the adsorbed layer.

I. Introduction

Polymeric chains adsorbed or grafted to an interface have been the subject of theoretical and experimental investigations in view of the numerous practical applications of the morphologies adopted by these chains. Surface polymer layers are encountered in steric stabilization of colloidal particles,[1−3] membrane systems,[4] adhesion technology,[5−8] and selective microphase separation.[9] Detailed studies of adsorbed polymer layers at the air−solution interface using neutron reflectivity have been reported.[10−12] For grafted chain layers, the structure and density profile have been investigated using small angle neutron scattering[13−16] and by specular neutron reflectivity.[17−25]

Our aim is to investigate the surface properties of a new type of nonadsorbing chains attached to the air−water interface by a few hydrophobic groups randomly localized on the chain. The polymer, cholesterylpullulan (CHP), is an associative polymer obtained by chemical modification of the naturally occurring polysaccharide pullulan produced by the fungus *Aureobasidium pullulans*. In the system investigated, the macromolecule has both hydrophobic head type attractions localized on the chain and a uniform repulsive interaction of the chain monomers with the surface. The number of anchoring points per chain lies between 1.7 and 4.5 depending on the degree of substitution of the derivatives.

The pullulan backbones are in good solvent conditions in water. Their solution properties as well as those of the hydrophobically modified CHP derivatives have been described by Kato et al.[26] and Nordmeier,[27] and by Akiyoshi et al.,[28−30] respectively. The use of CHP derivatives in the colloidal stabilization of vesicles is one of the potential applications of these biocompatible polymers. Grafted vesicles show very good colloidal stability[31] compared to the native unstabilized vesicles. However, the length of the adsorption kinetics at the air−water interface[31] and at spread lipid monolayers[32] makes it very difficult to observe the thermodynamic equilibrium of the system. Solubilization of these derivatives in lyotropic lamellar phases has also shown to be strongly time-dependent.[33,34] In this study, we will focus on the structural and the kinetic aspects in order to monitor the evolution of the layers with time.

II. Neutron Reflectivity

The principles and applications of neutron reflectivity have been reviewed by Russell[35] and by Penfold and Thomas.[36] Briefly, optical phenomena such as reflection and refraction at an interface apply also to neutrons. Neglecting absorption, for a given monochromatic neutron beam of wavelength λ, the neutron refractive index n of a material is given by[37]

$$n = 1 - \frac{\lambda^2 Nb}{2\pi} \tag{1}$$

where N is the number density of the material and b its coherent scattering length. The product Nb is the coherent scattering length density of the material. Using monochromatic neutrons with wavelength λ, total reflection of the beam is observed for any incident angle inferior to the critical angle θ_c, defined by

$$\theta_c = \lambda\left(\frac{Nb}{\pi}\right)^{1/2} \tag{2}$$

From this relationship, a variation of incident angle can be replaced by that of wavelength at a fixed incident angle, and we can define a critical wavelength by

$$\lambda_c = \theta\left(\frac{\pi}{Nb}\right)^{1/2} \tag{3}$$

In the *time-of-flight* technique, the reflecting liquid surface is illuminated by a polychromatic neutron beam at fixed incident

* Corresponding author.
[†] Service de Chimie Moléculaire. Present address: Institut Laue-Langevin, B.P. 156, 38042 Grenoble Cedex 9, France.
[‡] Laboratoire Léon Brillouin, CEA-CNRS.
[⊗] Abstract published in *Advance ACS Abstracts,* September 15, 1997.

S1089-5647(97)01432-6 CCC: $14.00

angle. A chopper is used to obtain a pulsed neutron beam. The beam is bent to the desired incident angle and the neutrons are detected after reflection from the sample, with a delay which is a function of their velocity. The *time-of-flight* of a neutron is the time elapsed between its emission and its detection. The wavelength of each neutron is determined according to

$$\lambda = \frac{ht}{mL} \tag{4}$$

where h is Planck's constant, t the time-of-flight, m the neutron mass, and L the chopper-to-detector distance (7.5 m at the DESIR reflectometer).

Specular reflection is determined by the mean scattering length density normal to the interface, and the reflectivity, R, is the ratio of the intensity of the specularly reflected beam (I_r) to that of the incident beam (I_i). For a sharp and structureless interface (Fresnel) where the refractive index varies as a step function from one medium to another, reflectivity is given by

$$R(\lambda) = \quad 1 \text{ for } \quad \lambda > \lambda_c \tag{5a}$$

and

$$R(\lambda) = \left[\frac{1 - [1 - (\lambda/\lambda_c)^2]^{1/2}}{1 + [1 - (\lambda/\lambda_c)^2]^{1/2}}\right]^2 \quad \text{for} \quad \lambda < \lambda_c \tag{5b}$$

In the presence of an interfacial structure such as a surface layer, the reflectivity is expressed as[38]

$$R(\lambda) = \frac{r_{12}^2 + r_{23}^2 + 2r_{12}r_{23}\cos(2\beta)}{1 + r_{12}^2 r_{23}^2 + 2r_{12}r_{23}\cos(2\beta)} \tag{6}$$

with

$$r_{ij} = \frac{n_i \sin\theta_i - n_j \sin\theta_j}{n_i \sin\theta_i + n_j \sin\theta_j} \tag{7}$$

and

$$\beta = \frac{2\pi}{\lambda} n_2 d_2 \sin\theta_2 \tag{8}$$

where r_{ij} is the Fresnel coefficient at the ij interface. The subscripts refer to air (1), the interfacial layer (2), and the substrate (3). d_2 is the thickness of the layer. This approach can be extended without too much difficulty to three or four discrete layers. However, when the profile is a smooth function, a popular method for calculating the reflectivity is to divide the surface layer into a finite number of uniform and discrete layers and calculating the Fresnel reflectance at each interface. In this case, one can apply the matrix formalism used in conventional optics for the calculation of multilayers where the elements of each layer are represented in a matrix form.[38] Multiplication of all the matrices results in a final two-by-two matrix, the elements of which describe the resulting reflectivity. In the present study, we have adopted this method to analyze the data. In the calculation of the Fresnel reflectivity, two corrections are included: the first originates from deviations due to the angular resolution of the spectrometer, and the second from the surface roughness. $R(\lambda)_{\theta,\Delta\theta,\sigma}$ is the calculated reflectivity for a given incident angle θ with a spread in angular resolution $\Delta\theta$ and a surface roughness σ. For simplicity, this function is denoted as $R(\lambda)$ or $R(k_z)$ when the reflectivity is given as a function of the perpendicular component of the wave vector, $k_z = (2\pi/\lambda)\sin\theta$.

III. Materials and Methods

1. Neutron Reflectometer. The experiments were performed at the DESIR TOF-reflectometer in the Orphée reactor (Laboratoire Léon Brillouin, Saclay). Reflectivity from the surface of the polymer solutions was performed in a Teflon trough placed in an enclosure with quartz windows transparent to the neutron beam. The trough has a surface of 75 cm^2 (15 cm × 5 cm) and a depth of 3 mm. Prior to each experiment the trough was cleaned in sulfochromic acid and abundantly rinsed in Milli-Q water. The trough was filled with the polymer solution and the surface cleaned by pipet aspiration.

2. Chemicals. The chemical structures of pullulan and CHP derivatives are given in Figure 1. A description of the pullulan and CHP samples are given in Tables 1 and 2, respectively. High molecular weight pullulan samples P_{360} and P_{1660} were supplied by Showa Denko (Tokyo, Japan). Low molecular weight pullulan samples P_{45}, P_{50}, and P_{52}, as well as $CHP_{45-0.6}$ and $CHP_{50-0.9}$ derivatives, were a gift from K. Akiyoshi.[39] The chemical modification is described elsewhere,[28] and the degree of substitution of the derivatives was determined by ^{1}H NMR. $CHP_{52-1.4}$ was supplied by Dojindo Laboratories (Kumamoto, Japan). As indicated in Table 2, $CHP_{52-1.4}$ is a derivative of molecular weight 52 000 with a degree of substitution of 1.4% (1.4 cholesterol group per 100 glucose units), corresponding to an average number of 4.5 cholesterol anchors per chain. The radius of gyration of pullulan was calculated according to[26]

$$R_g = 0.147 M_w^{0.58} \tag{9}$$

The critical bulk and interfacial overlap concentrations, C_p^* and Γ_p^*, respectively, are calculated according to[40]

$$C_p^* = \frac{3M_w}{4\pi N_A R_g^3} \tag{10}$$

and

$$\Gamma_p^* = \frac{M_w}{4N_A R_g^2} \tag{11}$$

The polymer solutions were prepared by sonication and heating under stirring (40 °C) until a clear solution was obtained. Water was produced by the Milli-Q water purification system from Millipore (Bedford, MA), and heavy water (deuterium enrichment 99.9%) was from Euriso-top (Saclay, France).

3. Scattering Length Density of the Polymer. The properties of the materials used in this study are given in Table 3. The scattering length densities of the polysaccharide and of the solvent are plotted Figure 2 as a function of the D_2O volume fraction in the solvent. Polysaccharides, like other biopolymers such as proteins, have a non-negligible content of weak acid hydrogen. In polysaccharides, these labile hydrogens are exclusively located on hydroxyl groups (Figure 2). Considering a random exchange between the solvent and the polymer and the same equilibrium constants for H/H and H/D exchanges, the deuterium enrichment of the labile sites is equal to the mole fraction of D_2O in the H_2O/D_2O mixture. The scattering length density of the polysaccharide can be calculated according to

$$Nb_p = Nb_{p,H} + \Phi_{D_2O}\left[n\frac{(b_D - b_H)}{191}\right] \tag{12}$$

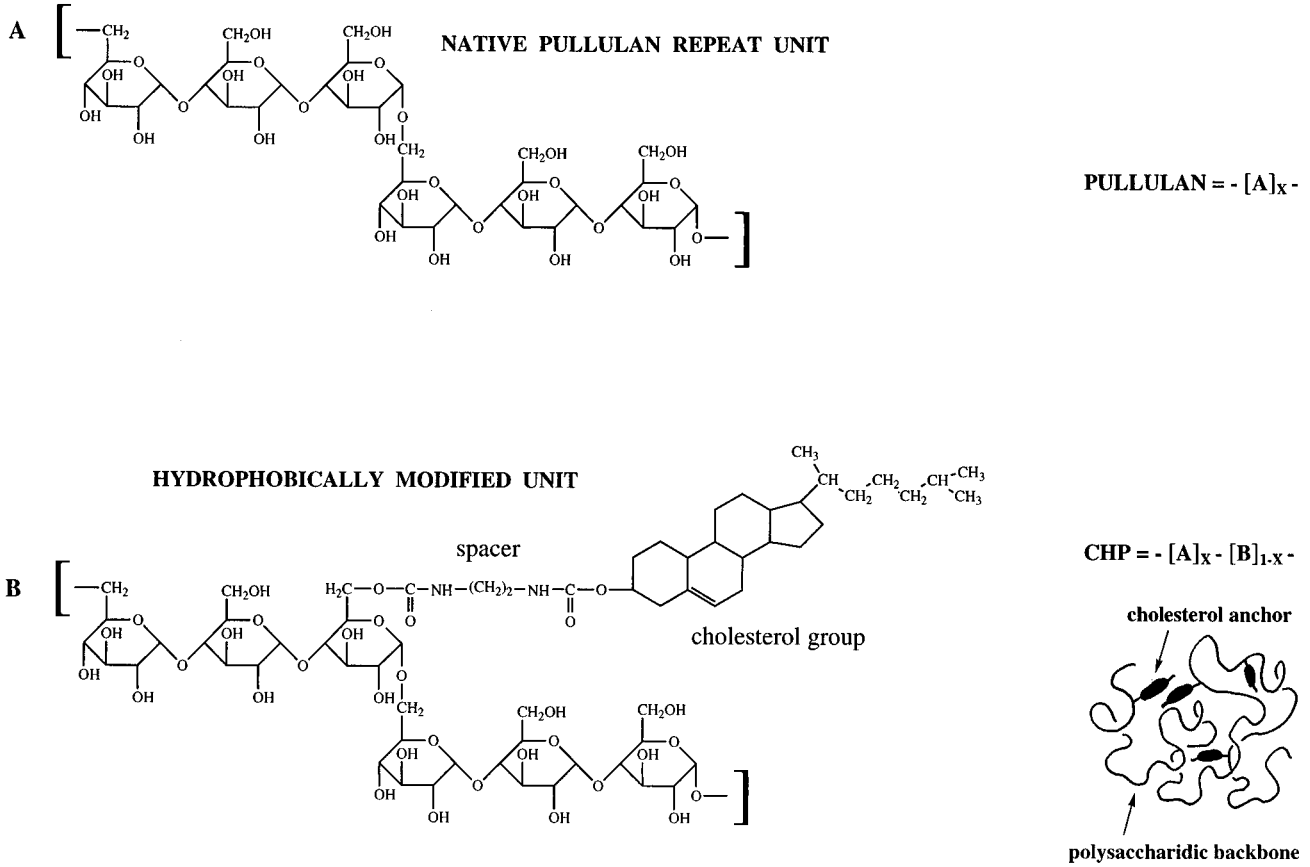

Figure 1. Chemical structure and schematic representation of pullulan and cholesterylpullulan derivatives (CHP). Pullulan is the native unmodified homopolysaccharide (A repeat unit), while the hydrophobically modified polysaccharide is a random copolymer of native A and modified B units bearing lateral cholesterol anchors.

TABLE 1: Description of Pullulan Samples[a]

pullulan	MW	M_w/M_n	R_g (Å)	C^* (g/L)
P_{45}	45 000	1.29	73	45
P_{50}	50 000	1.24	78	42
P_{52}	52 000	1.22	80	40
P_{300}	300 000	1.12	221	11
P_{1660}	1 660 000	1.19	596	3.1

[a] M_w/M_n values reported for the low molecular weight samples P_{45}, P_{50}, and P_{52} are results of HPLC−SEC analysis combined with low angle laser light scattering measurement. The values for P_{360} and P_{1660} were given by Showa Denko. The radii of gyration and the critical overlapping concentrations were calculated according to eqs 9 and 10, respectively.

TABLE 2: Description of CHP Samples[a]

CHP	MW	d.s. (%)	n_a	Γ^* (mg/m^2)
$CHP_{45-0.6}$	45 000	0.6	1.7	0.35
$CHP_{50-0.9}$	50 000	0.9	2.8	0.34
$CHP_{52-1.4}$	52 000	1.4	4.5	0.34

[a] The polydispersity of the polysaccharidic backbone in the CHP derivatives is the same as that reported in Table 1 for unmodified pullulan samples. The interfacial critical overlapping concentrations Γ^* were calculated according to eq 11.

where $Nb_{p,H}$ is the scattering length density of the polysaccharide in H_2O, i.e., completely protonated (1.65×10^{-6} Å^{-2}). n is the number of labile protons (3 per monomer); b_d and b_h are the scattering lengths of deuterium and hydrogen, respectively. In these calculations it is assumed that all hydrogen are accessible to the solvent for exchange. The ratio $(b_D - b_H)/191$ is the increment in scattering length density for each hydrogen exchanged by a deuterium in a monomer unit of volume $V = 191$ Å^3. In pure heavy water, $\Phi_{D_2O} = 1$, and $Nb_{p,D} = 3.29 \times 10^{-6}$ Å^{-2}. The scattering length density of the subphase is given by

$$Nb_s = Nb_{H_2O}\Phi_{H_2O} + Nb_{D_2O}\Phi_{D_2O} + Nb_{pol}\Phi_{pol} \quad (13)$$

In our experiments, the concentration of the polymer $\Phi_{CHP} \leq 0.1\%$ so that $\Phi_{H_2O} + \Phi_{D_2O} \approx 1$ and eq 13 simplifies to

$$Nb_s = Nb_{H_2O}(1 - \Phi_{D_2O}) + Nb_{D_2O}\Phi_{D_2O} \quad (14)$$

For the same reason, we also neglect the change in scattering length density of the solvent due to H enrichment by the polysaccharide.

4. Scattering Length Density Contrast. A simplified view of the scattering length density profile in the presence of an adsorbed CHP layer is given in Figure 3 for the contrast obtained with the protonated polymer in pure D_2O ($Nb = 6.37 \times 10^{-6}$ Å^{-2}). The adsorbed polymer layer is arbitrarily represented by a step function for simplicity. A schematic representation of the adsorbed polymer with the hydrophobic cholesterol groups anchored at the interface is also shown in the figure. Due to the high hydrogen content of the cholesterol, the scattering length density of the anchors is very low (0.22×10^{-6} Å^{-2}). Furthermore, the degree of substitution of the CHP derivatives is such that the enrichment of the interface by cholesterol groups must be very low, the limiting parameter in forming a condensed phase of cholesterol groups being the size of the swollen polysaccharidic backbones. The scattering length density of the cholesterol layer in the air phase is certainly much lower than that of a pure condensed cholesterol layer (0.22×10^{-6} Å^{-2}). Therefore the contribution of the cholesterol layer to the total reflectivity signal was considered to be negligible. As indicated

TABLE 3: Properties and Data Used for the Calculations of the Scattering Length Density of the Materials

material	formula	M (g mol^{-1})	ρ (g cm^{-3})	b^b ($\times 10^4$ Å)	V (Å^3)	Nb ($\times 10^6$ Å^{-2})
water	H_{2O}	18	0.997[a]	−0.168	30	−0.56
heavy water	D_{2O}	20	1.105[a]	1.915	30	6.37
cholesterol	$C_{27}H_{45}OH$	387	1.067[a]	1.322	602	0.22
pullulan in H_2O	$-(C_6H_{10}O_5)_n-$	162	1.54	3.15	191	1.65
pullulan in D_2O	$-(C_6H_7D_3O_5)_n-$	165	1.57	6.28	191	3.29

[a] Taken from ref 53. [b] Taken from ref 54.

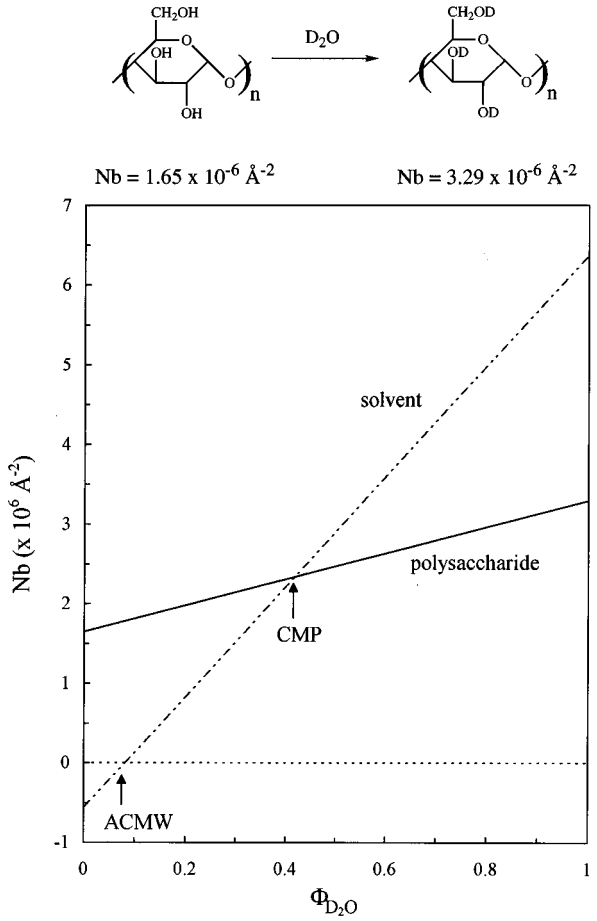

Figure 2. Exchange of labile H from glucose monomer units with the solvent and the consequence on the scattering length density of the polymer. The plot is a calculation of the scattering length density of the polymer as a function of the solvent composition in H_2O/D_2O mixtures. We use eqs 12 and 14 for the polymer and the solvent, respectively. Equation 14 applies to dilute solutions where the enrichment of the solvent by hydrogen from the polymer may be neglected. ACMW = air contrast matched water; CMP = contrast matched point of the polymer.

in Figure 2, exchange of labile hydrogen with the deuterated solvent results in an increase in the scattering length density of the polymer from 1.65×10^{-6} Å^{-2} to 3.29×10^{-6} Å^{-2}, reducing the scattering length density contrast from -4.72×10^{-6} Å^{-2} to -3.08×10^{-6} Å^{-2}.

IV. Results

1. Native Pullulan Solutions. Nonmodified pullulan showed no measurable adsorption from dilute solutions at the air−solution interface. The reflectivity curves superpose with the pure D_2O curve. There is also no detectable depletion of a polymer at the surface. This is not surprising since the experimental conditions employed here are not sufficiently sensitive to detect the possible existence of such a layer, due to the weak contrast between the dilute polymer solutions and the pure solvent. Indeed, it has been shown that depletion layers

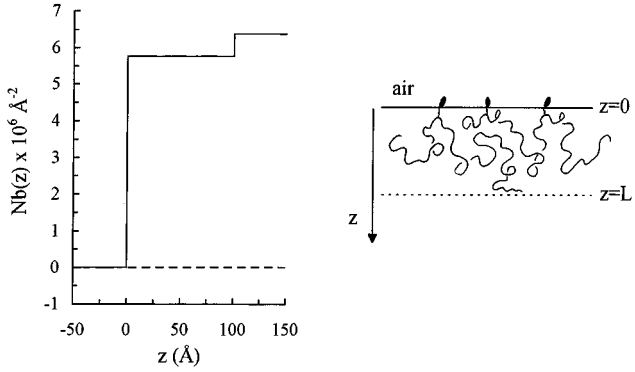

Figure 3. Scattering length density contrast and schematic representation of the adsorbed CHP derivative from a D_2O solution. The profile is represented by a step function for simplicity. Note that adsorbed cholesterol groups at the air−water interface are quasi-contrast matched to the air ($Nb \leq 0.22 \times 10^{-6}$ Å^{-2}). $Z = 0$ corresponds to the cholesterol−water interface as indicated in the scheme.

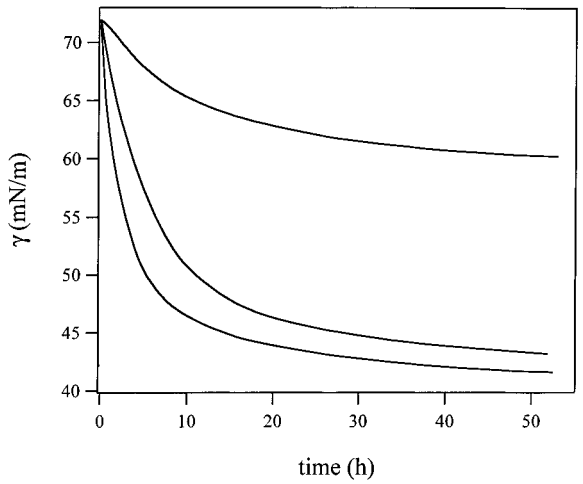

Figure 4. Surface tension curves of $CHP_{52-1.4}$ from D_2O solutions. From top to bottom: $C_p = 0.25$, 0.50, and 1.0 g/L.

are more easily observed under semidilute solution conditions.[41] These results are in agreement with the absence of any surface activity controlled by surface tension experiments on aqueous pullulan solutions.[31]

2. Modified CHP Solutions. Modified pullulan, however, shows considerable surface activity. The dynamic surface tensions shown in Figure 4 for three concentrations of $CHP_{52-1.4}$ show that very long times are required for equilibrium to be achieved. Such long equilibration times have also been reported for other water soluble polymers carrying hydrophobic moieties.[42−44]

Reflectivity profiles by $CHP_{52-1.4}$ solutions at $C_p = 0.05$, 0.25, and 1.0 g/L in D_2O are shown in Figure 5. The dotted lines are calculated Fresnel reflectivity for pure D_2O where the refractive index varies as a step function from the air to the bulk with a roughness of 3 Å, although the latter is not measurable in the range of wave vector used in the experiments. For the polymer solutions, small but detectable deviations from

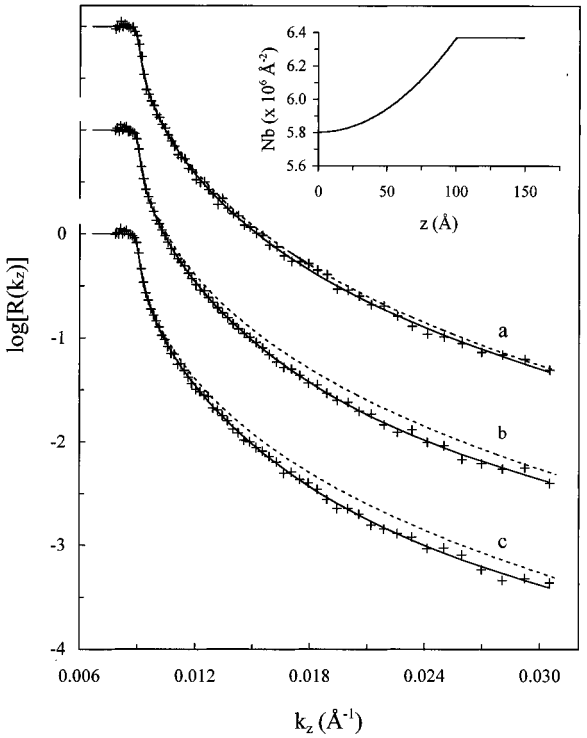

Figure 5. Reflectivity curves obtained with $CHP_{52-1.4}$ adsorbed from dilute D_2O solutions at $C_p = 0.05$ g/L (curve a), 0.25 g/L (curve b), and 1.0 g/L (curve c). The dotted lines are calculated Fresnel curves, and the solid lines correspond to the best fits calculated using the parabolic profile given in eq 15. Inset: scattering length density profile corresponding to the calculated curve for 1.0 g/L.

the reflectivity by the pure solvent are observed. The solid lines represent the best fits calculated with the type of scattering length density profile shown in the inset. In these experiments, although the deviations of the reflectivity profiles from the Fresnel curve are small, they are certainly measurable. The relatively low reflectivity signals observed here are common for swollen protonated polymer layers adsorbed form a deuterated solvent, as already reported by Guiselin et al. for protonated poly(dimethysiloxane) adsorbed from deuterated toluene at the free surface.[11,12] In their case, using different contrast variation schemes by combinations of protonated and deuterated polymers and solvents, and by simultaneous analyses of numerous series of data obtained for several polymer concentrations and chain lengths, they were able to obtain an unequivocal segment density profile to describe the adsorbed layer.[12] In our case, with the lack of deuterated polymer, our aim is not to obtain a unique profile. Rather, we determine, among a series of selected profiles, the profile that best fits the data, and using that profile, we investigate the average structures of the adsorbed layers and their evolution with different physical parameters.

3. Concentration Profiles of the Adsorbed Polymer Layers. We have tested a series of model concentration profiles that include the step, parabolic, half-Gaussian, and power law profiles. The efficiency of the models was controlled by comparison of the fits with experimental data and by χ^2 analysis. Of these profiles, the power law density decay ($\Phi_p(z) \sim z^{-4/3}$) predicted by scaling theories for homopolymers adsorbed from good solvents[45] and verified experimentally by neutron reflectivity[12] gave the worst fits: for $CHP_{52-1.4}$ at 0.25 g/L, $\chi^2 = 5.46$. The corresponding value using a parabolic function is $\chi^2 = 1.36$. Other profiles that gave intermediate fits are shown in Figure 6. However, when tested for all other concentrations of the $CHP_{52-1.4}$ derivative and for two other CHP samples having degrees of substitution of 0.9 and 0.6%, only the parabolic

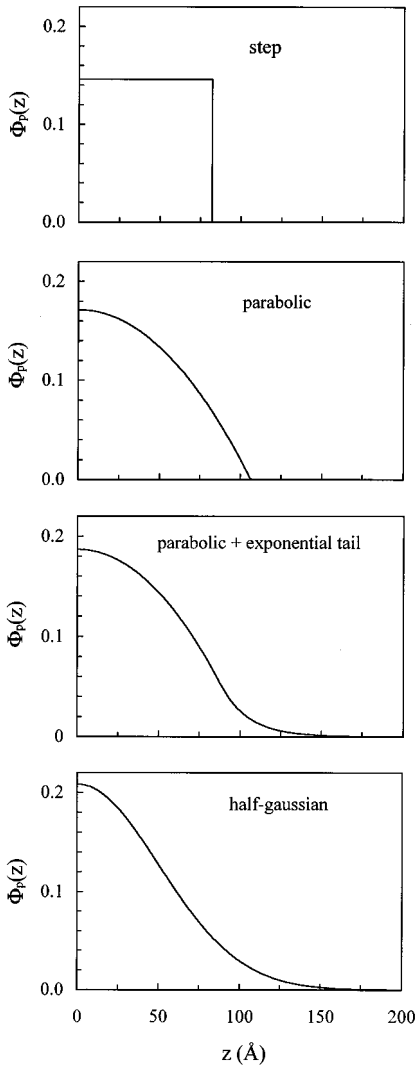

Figure 6. Representation of the concentration profiles tested for the adsorbed layers.

profile gave consistently good fits in all the cases; typical values of χ^2 are in the range 0.85−1.36. The results of the fits are given in Table 4 for three $CHP_{52-1.4}$ concentrations. The corresponding profiles are given in Figure 7.

Note that in our case a simple parabolic profile yields the best fit. This is in contrast to end-attached chains where an exponential tail is required to fit the data at moderate surface concentrations.[24] For the same reason, the half-Gaussian model did not give a better fit. The addition of a depletion layer to the surface region did not improve the quality of the fits either. The depletion layer has been tested since the polysaccharidic backbone is supposed to have a repulsive interaction with the interface, but the failure to detect this depletion layer could be due to insufficient contrast, as mentioned above.

The values of polymer surface excess Γ_p (mg/m^2) reported in Table 4 have been calculated by integrating the parabolic concentration profile:

$$\Phi_p(z) = \Phi_s\left[1 - \left(\frac{z}{L}\right)^2\right] \tag{15}$$

where Φ_s is the surface concentration of the polymer ($\Phi_s = \Phi_p(z=0)$), and L the thickness of the polymer layer defined by the parabolic function. The adsorption is then

$$\Gamma_p = (0.1)\rho\int_0^{\infty}\Phi_s\left[1 - \left(\frac{z}{L}\right)^2\right] \tag{16}$$

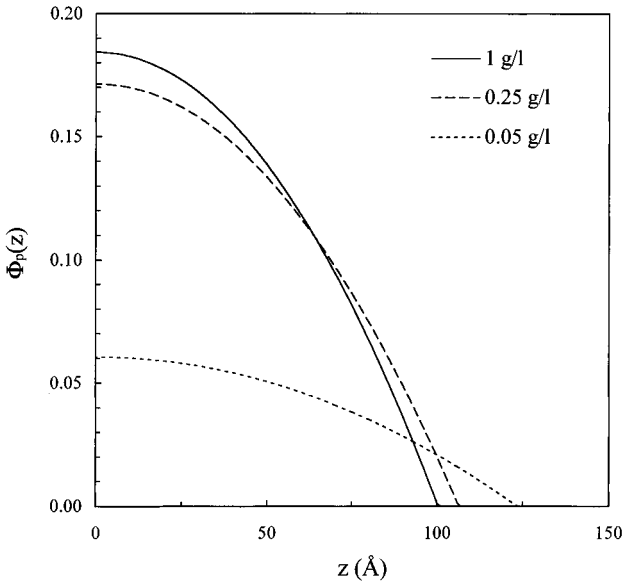

Figure 7. Comparison of the parabolic concentration profiles obtained for three $CHP_{52-1.4}$ concentrations: 0.05 g/L (dotted curve), 0.25 g/L (dashed curve), and 1.0 g/L (solid curve).

TABLE 4: Fitted and Calculated Parameters Describing the $CHP_{52-1.4}$ Layers[a]

[CHP] (g/L)	Φ_s (v/v)	L (Å)	Γ_p (mg/m^2)	L/R_g
0.05	0.07	125	0.8	1.56
0.25	0.17	106	1.9	1.32
1.00	0.19	100	2.0	1.26

[a] Φ_s is the chain surface concentration in the proximal region (z = 0), and L the thickness of the concentration profile defined by the parabolic function. Γ_p is calculated according to eq 17. The ratio L/R_g shows the degree of the chain stretching. The concentration profiles corresponding to these data are given in Figure 8.

At $z = \infty$, we have $\Phi_p(z{=}\infty) = \Phi_{bulk}$, and neglecting Φ_{bulk} we can integrate from $z = 0$ to $z = L$, giving

$$\Gamma_p = (0.1)\rho\frac{2}{3}\Phi_s L \qquad (17)$$

where ρ is the melt density.

4. Effect of Polymer Solution Concentration. Figure 7 shows the concentration profiles obtained for three concentrations of $CHP_{52-1.4}$ (see Table 4 for the fitted parameters). These profiles show that as the polymer solution concentration is increased, the surface concentration $\Phi_s = \Phi_p(z{=}0)$ increases while the thickness of the adsorbed layer, L, shows a small decrease. Note that the polymer layer is saturated at a concentration in the vicinity of aggregation formation in the solution (~0.4 g/L).[31]

5. Effect of Degree of Substitution. A comparison of the concentration profiles obtained with the three CHP samples differing in their degree of substitution at $C_p = 0.25$ g/L is given in Figure 8. The extension of the profile has been normalized to the radius of gyration of the polymer in order to take into account the small differences in molecular weights. The corresponding fitted parameters are reported in Table 5. Clear trends are observed: Φ_s, L and Γ_p decrease with increase in degree of substitution.

6. Adsorption Kinetics. To resolve the structure of the layers during the adsorption kinetics, we have reduced the acquisition period to 3 h. The results obtained with $CHP_{52-1.4}$ at 0.5 g/L are reported in Figure 9. We have plotted the variations with time, of L, Φ_s, and Γ_p resulting from the parabolic fits, as well as the surface tension of the polymer solution. One can see that even though L, Φ_s, and the surface tension continue to vary over time, the adsorption density, Γ_p, remains constant. These data show that the adsorbed polymer layer is condensed, at a constant surface excess, over time.

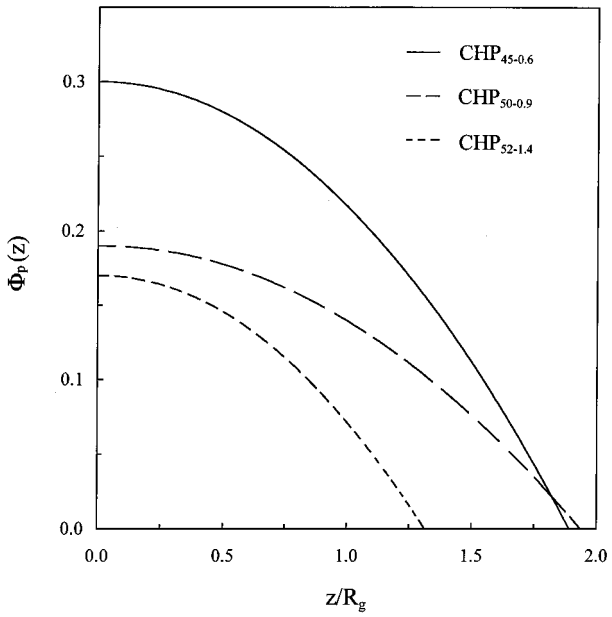

Figure 8. Comparison of the parabolic concentration profiles obtained for the three CHP derivatives with varying degree of substitution at C_p = 0.25 g/L: $CHP_{45-0.6}$ (solid curve), $CHP_{50-0.9}$ (long dash curve), and $CHP_{52-1.4}$ (short dash curve). The extension of the profile is normalized with respect to the radius of gyration of the chain to take into account the differences in molecular weight of the three derivatives.

TABLE 5: Comparison of Surface Properties of the Three CHP Derivatives Investigated[a]

derivative	n_a	Φ_s (v/v)	L (Å)	Γ_p (mg/m^2)	L/R_g
$CHP_{45-0.6}$	1.7	0.30	140	4.3	1.89
$CHP_{50-0.9}$	2.8	0.19	150	3.0	1.92
$CHP_{52-1.4}$	4.5	0.17	106	1.9	1.32

[a] The derivatives differ in their degree of substitution from 0.6 to 1.4%. The subphase concentration is 0.25 g/L.

7. Temperature Effect. The thickness of the polymer layers has been plotted as a function of the polymer surface excess in Figure 10. All reported values of Γ_p are higher than the critical overlap concentration of $CHP_{52-1.4}$ (dotted line). The chains in the adsorbed layer are slightly stretched ($1.26 < L/R_g < 1.56$), but the stretching decreases with Γ_p. The temperature dependence shows the effect of the solvent quality: an increase in temperature causes a deswelling of the polymer layer, indicating a possible upper critical temperature in which the polymer is in θ condition. At the two temperatures investigated, we observe a decrease in the layer thickness with Γ_p. This result is in opposition to theoretical predictions[46−51] and experimental observations of chain stretching for end-attached tethered polymer layers.[13−15,21−25] The concentration dependence of the layer thickness is more pronounced at 25 °C than at 20 °C, and the difference between the thickness more significant at low surface excess.

V. Discussion

Native pullulan is a hydrophilic polysaccharide that does not exhibit any surface activity. However, when small amounts of hydrophobic cholesterol groups are grafted onto the polymer backbone, hydrophobic and associative characteristics are imparted to the chain, rendering it surface active. In addition, if the grafting density of the cholesterol groups is high enough,

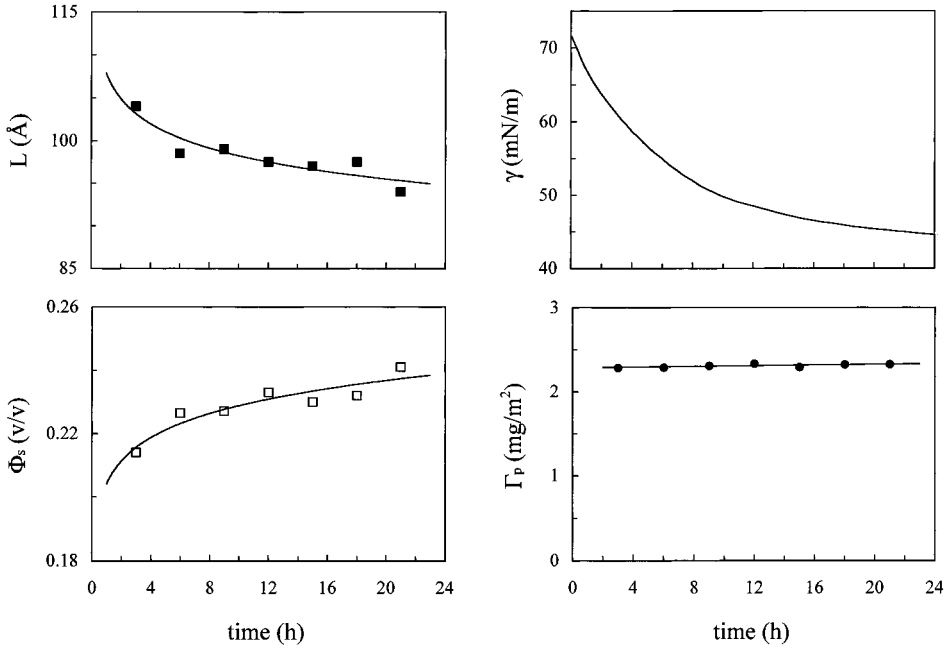

Figure 9. Evolution of L, Φ_s, Γ_p, and γ as a function of time for $CHP_{52-1.4}$ at $C_p = 0.5$ g/L.

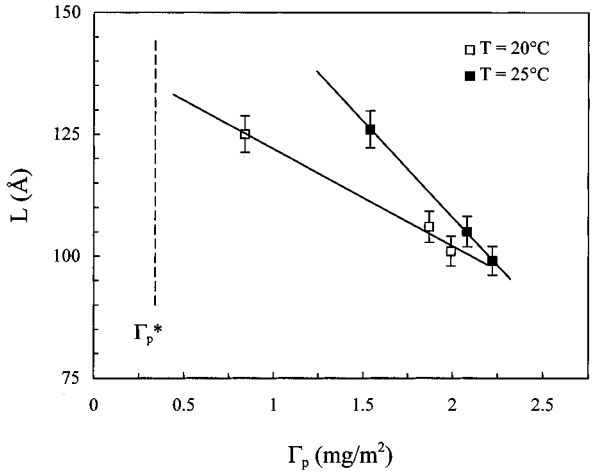

Figure 10. Dependence of the polymer layer thickness L with the surface excess Γ_p for $CHP_{52-1.4}$ layers adsorbed from dilute solutions at two temperatures. The polymer chains in the adsorbed layer are in the semidilute regime ($\Gamma_p > \Gamma^*$).

aggregation of the chains takes place, a phenomenon similar to micelle formation observed in surfactant solutions. Experimentally, the onset of such aggregation is manifested as a break in the slope of the surface tension curve.[31]

When the surface activity of CHP at the air−water interface is monitored by surface tension measurements, several characteristics can be noted. First, a very long equilibration time is apparently required for the formation of the adsorbed polymer layer. In addition, this approach to equilibrium state is concentration dependent: the more dilute the solution concentration, the longer it takes to reach equilibrium. Such long adsorption times have also been observed for other hydrophobic polymers[42−44] and have been explained in terms of reconfiguration of the adsorbed layer.[42]

Surface tension data alone do not give access to a complete profile of the adsorbed layer, therefore, the maximum adsorbed amount cannot be deduced. In fact, for polymer solutions, it is proposed that only those segments in direct contact with the surface contribute to the change in surface tension.[42,52] For adsorption of homopolymers from a dilute solution, this monomer-rich proximal zone[45] is only a few angstroms thick. Within this zone, surface potential and short-range monomer−surface interactions are felt. As a result, the properties within this zone, in terms of the structure and the surface tension, should be independent of the polymer chain length. This has been shown experimentally to be true from surface tension and neutron reflectivity measurements.[11,12] A theoretical discussion of the universality of this zone has also been reported.[52]

In the present study, our neutron reflectivity data show that, indeed, surface tension measurements are sensitive to the surface zone and therefore do not reflect precisely the total amount of polymer adsorbed. For $CHP_{52-1.4}$ at 0.5 g/L, neutron reflectivity data show that saturation is achieved within 3 h (the adsorption density remains constant from 3 to 21 h) even though the surface tension continues to decrease over the same period of time. On the other hand, L and Φ_s continue to vary with time, showing an evolution of the structure of the adsorbed layer, which becomes thinner and more concentrated at the surface. We attribute this slow structural rearrangement to the adsorption of the cholesterol groups in the subsurface: after the rapid adsorption of the chains by a few anchored cholesterol groups, free cholesterol groups attached to the chain but not yet adsorbed may continue to adsorb at the interface. This step requires considerable time since the cholesterol groups have to diffuse in the polymer network to reach the interface. As more cholesterol groups are adsorbed, polymer chains are brought closer to the interface (decrease in the loop size), resulting in a decrease in the layer thickness and an increase in the surface density. The equilibrium state of the system may be described by entangled chains whose interpenetration is the result of the paths taken by the cholesterol groups during the diffusion step in the network.

The results reported in Figure 8 and Table 5 show the effect of the degree of substitution of the chain, i.e., the number of cholesterol groups randomly localized on the polysaccharidic backbone. It is interesting to compare the surface excess of $CHP_{45-0.6}$, $CHP_{50-0.9}$ and $CHP_{52-1.4}$: note that a high degree of substitution is not required to obtain a high surface excess. On the contrary, the lowest degree of substitution gives the highest adsorption density. This can be explained by the fact that an increase in the degree of substitution reduces the distance between the anchors on the chain, thus reducing the lengths of

the polymer loops and tails. Consequently, the overall thickness of the layer and the total amount adsorbed are decreased. Another noteworthy feature is that the surface pressure of the films at equilibrium is not related to Γ_p nor to ϕ_s, but to the degree of substitution on the polymer backbone: the higher the degree of substitution, the lower the equilibrium surface tension.[31] This is in contrast to the case of adsorbed homopolymers where the final surface tension is related to the polymer-rich zone (ϕ_s) even though it is not related to Γ_p due to the extended loops and tails of the adsorbed layer. We propose, therefore, that the final surface pressure obtained in this system is due to the adsorption of cholesterol groups, and not to the polymer chain density in the vicinity of the interface.

The possibility of aggregation of nonadsorbed cholesterol groups in the polymer layer should not be neglected. As the cholesterol concentration is increased in the layer, due either to an increase in polymer concentration or to an increase in degree of substitution, the probability of interactions of the cholesterol groups is increased, and this may induce a condensation of the layer. This could explain the absence of chain stretching when the concentration of the chains at the interface is increased. If we calculate the number of cholesterol groups in the polymer layer by

$$\Gamma_c = \frac{\Gamma_p}{M_w} n_a \qquad (18)$$

where Γ_p is the total amount of adsorbed polymer, M_w its molecular weight, and n_a the number of cholesterol anchors per chain, we obtain the same amount of cholesterol, 162, 168, and 164 μg/m^2 for $CHP_{45-0.6}$, $CHP_{50-0.9}$ and $CHP_{52-1.4}$, respectively. If all these cholesterol groups were adsorbed at the surface, one would expect the final pressures to be the same for all three CHP samples. However, the significant differences observed in the pressures suggest that the cholesterol molecules are in fact adsorbed in different amounts for different degrees of substitution.

VI. Conclusion

Non surface active polysaccharide macromolecules can be adsorbed to the air−water interface by hydrophobic cholesterol groups grafted along the backbone of the polymer. In dilute solutions, the adsorbed layer is very slightly stretched, and the total adsorbed amount varies between that expected of adsorbed homopolymers (1−2 mg/m^2) and that of grafted layers at moderate density (several mg/m^2). The polymer molecule is pictured to be adsorbed in loops, with each loop attached to the surface at both ends by the cholesterol groups. The further apart the cholesterol groups are spaced, the longer the loops that are formed, resulting in thicker adsorbed layers and higher adsorption density. Thus, the adsorbed layer thickness and the adsorption density decrease with the number of hydrophobic anchoring groups per chain.

Surface tension measurements coupled with neutron reflectivity data show that the long equilibration times observed for the formation of the polymer layers are due to structural rearrangement in the adsorbed layer, while the total amount adsorbed remains constant: over time, the adsorbed layer becomes thinner and more condensed. This is attributed to the diffusion of the cholesterol groups in the polymer network of adsorbed layer to the interface. The associative properties of these hydrophobic groups within the surface polymer layer may also play a role in condensing the polymer layer.

Acknowledgment. B.D. is grateful to B. Cabane for his help in initiating this study. We would like to thank H. Maréchal (Showa Denko Europe) for supplying free pullulan and P. Lixon for the HPLC analysis of the samples. We are indebted to I. Iliopoulos for helpful and critical discussions. B.D. was supported by a grant of the French Research Ministry. Pr. F. Puisieux is acknowledged for making this support possible.

References and Notes

(1) Ash, S. *Chem. Soc. Spec. Publ.: Colloid Sci*. **1973**, *1*, 103.
(2) Vincent, B. *Adv. Colloid Interface Sci*. **1974**, *4*, 193.
(3) Napper, D. H. *Polymeric Stabilization of Colloidal Dispersions*; Academic Press: London, 1983.
(4) Hair, M. *The Chemistry of Biosurfaces*; Marcel Dekker: New York, 1971; Vols. 1 & 2.
(5) Stromberg, R. In *Treatise on Adhesion and Adhesives*; Patrick, R., Ed.; Marcel Dekker: New York, 1967; Vol. 1.
(6) Lee, L. H. *Adhesion Science and Technology*; Plenum: New York, 1975.
(7) Smith, J. W.; Kramer, E. J.; Xiao, F.; Hui, J.; Reichharts, W.; Brown, H. *J. Mater. Sci*. **1993**, *28*, 4234.
(8) Smith, J. W.; Kramer, E. J.; Mills, P. J. *J. Polym. Sci.: Polym. Phys*. **1994**, *32*, 1731.
(9) Hennion, M.; Picart, C.; Caude, M.; Rosset, R. *Analysis* **1978**, *6*, 369.
(10) Rennie, A. R.; Crawford, R. J.; Lee, E. M.; Thomas, R. K.; Crowley, T. L.; Roberts, S.; Qureshi, M. S.; Richards, R. W. *Macromolecules* **1989**, *22*, 3466.
(11) Lee, L. T.; Guiselin, O.; Farnoux, B.; Lapp, A. *Macromolecules* **1991**, *24*, 2518.
(12) Guiselin, O.; Lee, L. T.; Farnoux, B.; Lapp, A. *J. Chem. Phys.* **1991**, *95*, 4632.
(13) Auroy, P.; Auvray, L.; Léger, L. *Phys. Rev. Lett.* **1991**, *66*, 719.
(14) Auroy, P.; Auvray, L.; Léger, L. *Macromolecules* **1991**, *24*, 5158.
(15) Auroy, P.; Auvray, L. *Langmuir* **1994**, *10*, 225.
(16) Cosgrove, T.; Heath, T. G.; Ryan K. *Langmuir* **1994**, *10*, 3500.
(17) Satija, S. K.; Majkrzak, C. F.; Russell, T. P.; Sinha S. K.; Sirota E. B.; Hughes, G. J. *Macromolecules* **1990**, *23*, 3860.
(18) Cosgrove, T.; Heath, T. G.; Phipps, J. S.; Richardson, R. M. *Macromolecules* **1991**, *24*, 94.
(19) Field, J. B.; Toprakcioglu, C.; Ball, R. C.; Stanley H. B.; Dai, L.; Barford W.; Penfold, J.; Smith, G.; Hamilton W. *Macromolecules* **1992**, *25*, 434.
(20) Field, J. B.; Toprakcioglu, C.; Hadziioannou, G.; Smith, G.; Hamilton W. *J. Phys. II* **1992**, *2*, 2221.
(21) Kent, M. S.; Lee, L. T.; Farnoux, B.; Rondelez F. *Macromolecules* **1992**, *25*, 6240.
(22) Kent, M. S.; Lee, L. T.; Factor B. J.; Rondelez F.; Smith, G. S. *J. Phys. IV* **1993**, *8*, 49.
(23) Factor B. J.; Lee, L. T.; Kent, M. S.; Rondelez F. *Phys. Rev. E* **1993**, *48*, 2354.
(24) Kent, M. S.; Lee, L. T.; Factor B. J.; Rondelez F.; Smith, G. S. *J. Chem. Phys.* **1995**, *103*, 2320.
(25) Kent, M. S.; Factor B. J.; Satija, S.; Gallagher, P.; Smith, G. S. *Macromolecules* **1996**, *29*, 2843.
(26) Kato, T.; Katsuki, T.; Takahashi, A. *Macromolecules* **1984**, *17*, 1726.
(27) Nordmeier, E. *J. Phys. Chem*. **1993**, *97*, 5770.
(28) Akiyoshi K.; Yamaguchi S.; Sunamoto, J. *Chem. Lett*. **1991**, 1263.
(29) Akiyoshi, K.; Sunamoto, J. In *Organized Solutions - Surfactants in Science and Technology*; Marcel Dekker: New York, 1992; p 289.
(30) Akiyoshi, K.; Deguchi, S.; Moriguchi, N.; Yamaguchi, S.; Sunamoto, J. *Macromolecules* **1993**, *26*, 3062.
(31) Demé, B. Thesis, Université Paris XI, Orsay, 1995.
(32) Demé, B. Unpublished results.
(33) Demé, B.; Dubois, M.; Zemb Th.; Cabane, B. *J. Phys. Chem.* **1996**, *100*, 3828.
(34) Demé, B.; Dubois, M.; Zemb Th.; Cabane, B. *Colloids Surf. A* **1997**, *121*, 135.
(35) Russell, T. P. *Mater. Sci. Rep.* **1990**, *5*, 171.
(36) Penfold, J.; Thomas, R. K. *J. Phys. Condens. Matter* **1990**, *2*, 1369.
(37) Werner, S. A.; Klein, A. G. In *Neutron Scattering*; Skold, K., Price, D. L., Eds.; Academic Press: New York, 1986.
(38) Born, M.; Wolf, E. *Principles of Optics*; Pergamon Press: Oxford, 1975.
(39) Laboratory of Materials Science of Polymers and Artificial Cell Technology, Department of Polymer Chemistry, Kyoto University.
(40) Des Cloizeaux, J.; Jannink, G. *Les Polymères en Solution: Leur Modélisation et Leur Structure*; Les Editions de Physique: Les Ulis, France, 1987.
(41) Lee, L. T.; Guiselin, O.; Lapp, A.; Farnoux, B. *Phys. Rev. Lett*. **1991**, *67*, 2838.
(42) Lankveld, J. M. G.; Lyklema, J. *L. Colloid Interface Sci*. **1972**, *41*, 454.

(43) Chang, S. A.; Gray, D. G. *J. Colloid Interface Sci*. **1978**, *67*, 255.
(44) Nahringbauer, I. *J. Colloid Interf. Sci*. **1995**, *176*, 318.
(45) de Gennes, P.-G. *Macromolecules* **1981**, *14*, 1637.
(46) Alexander, S. *J. Phys. (Paris)* **1977**, *38*, 983.
(47) de Gennes, P.-G. *Macromolecules* **1980**, *13*, 1069.
(48) Cosgrove, T.; Heath, T.; van Lent, B.; Leermakers, F.; Scheutjens, J. J. M. S. *Macromolecules* **1987**, *20*, 1692.
(49) Milner, S. T.; Witten, T. A.; Cates, M. E. *Europhys. Lett.* **1988**, *5*, 413.
(50) Milner, S. T.; Witten, T. A.; Cates M. E. *Macromolecules* **1988**, *21*, 2610.
(51) Zhulina, E. B.; Borisov, O. V.; Pryamitsin, V. A. *J. Colloid Interface Sci.* **1990**, *137*, 495.
(52) Des Cloizeaux, J. *J. Phys. (Paris)* **1988**, *49*, 699.
(53) Weast, R. C. *Handbook of Chemistry and Physics*, 51st ed.; CRC Press: Cleveland, OH, 1970−1971.
(54) Sears, V. F. *Neutron News* **1993**, *3*, 26.